Crashworthiness Simulation Using Coupled Meshfree/Finite Element Formulations in LS-DYNA

Hui-Ping Wang, Ye-Chen Pan and Yi-Pen Cheng
General Motors Corporation

Abstract

This paper demonstrates applications of a coupled meshfree/finite element solver of LS-DYNA in the analysis of crashworthiness components. Two examples are employed in the study. The first one is a European side impact dummy component test problem. It is used to show the robustness of the coupled meshfree/finite element solver in handling large deformation since the finite element analysis of this problem fails due to numerical instability caused by negative element volume. By applying the meshfree formulation to the large distortion area, we successfully complete the simulation and obtain very reasonable solutions. The second problem is an engine cradle drop tower test. Various background meshes are created for this problem to study the effect of different element connectivity on accuracy of the meshfree solutions. The study shows that, with the same particle distributions the meshfree analysis yields more consistent solutions than the finite element analysis when the background connectivity varies.

Introduction

Today's vehicle development process heavily relies on computer-aided engineering (CAE) analysis. In most scenarios, the CAE analysis provides quick and accurate assessment of newly designed vehicle components and systems in terms of their manufacturability and targeted performance. Also, it helps to improve the design by virtually adjusting design parameters and verifying the models. With usage of the CAE analysis, expensive and time-consuming physical tests have been greatly reduced nowadays. Still, there are scenarios current CAE technologies cannot well comprehend. Exemplary problems are events and processes involving severe deformation, material separation, fluid-solid interaction, phase changing and other complex physics. Many researches are still going on in these fields searching for improved solutions.

One of the obstacles limiting current CAE tools' capability is the mesh quality problem. The finite element (FE) method employed in the CAE tools models the physical domain with discrete, non-overlapping conforming meshes. The order of finite element approximation constructed on each element degenerates when the element has aspect-ratio or geometric distortion. Consequently, the accuracy of the FE-based CAE analysis degrades or even fails. This often occurs in the simulations involving large deformation and shape change. Many researches have therefore been proposed on mesh adaptation and remeshing in order to maintain the mesh quality during the deformation process.

Meshfree methods were also proposed and developed to resolve this difficulty. Typical meshfree methods are Element Free Galerkin Method, Reproducing Kernel Particle Method, HP-clouds method and Partition of Unity method [1-6]. The main idea in these methods is to approximate field variables without usage of element connectivity. Meshfree methods construct their approximation functions on discrete particles, then apply them in approximating the field variables, and hence solve corresponding math models. Representative meshfree approximations are moving least square approximation and reproducing kernel approximation. These functions usually have high order smoothness and can exactly approximate high order polynomials.

Applications of these approximations in solving nonlinear large deformation or material separation problems [4, 7-8] show their great advantages over finite element methods in terms of model adaptivity and solution accuracy. However, meshfree methods consume much higher CPU than the FE methods, which greatly limits their applications in solving large-scale industrial problems.

Since in most problems large deformation or shape change only occurs locally, application of the meshfree approximation on whole problem domain becomes too expensive and unnecessary. Naturally, the idea of coupling meshfree methods with existing finite element methods was proposed by Huerta et al [9], and opened a door for the meshfree methods to be applied in solving large-scale problems. To make the meshfree method available and affordable, as a collaborative effort between GM and LSTC, the coupled meshfree/finite element method was further developed for industrial usage and implemented into LS-DYNA. The coupled meshfree/finite element solver for explicit dynamic simulation is now available in LS-DYNA v971.

In this paper, we will briefly review the coupled meshfree/finite element formulation. Then we will apply the coupled solver into two crash component analyses. The first one is a European side impact dummy component test problem. It is used to test the robustness of the coupled meshfree/finite element solver in terms of resolving element distortion difficulty since the finite element analysis of this problem fails due to element distortion. The second problem is an engine cradle drop tower test. It is used to study the sensitivity of the coupled solver with respect to various background element connectivity.

Coupled Meshfree/Finite Element Formulation

In the coupled method, the problem domain Ω is divided into finite element approximation zones and meshfree approximation zones, as shown in Figure 1. That is,

$\Omega = \sum_{i=1}^{nf} \Omega_{FEM}^{i} \cup \sum_{i=1}^{nm} \Omega_{meshfree}^{i}$, where *nf* is number of finite element zones and *nm* is number of

meshfree zones. The finite element zones consist of non-overlapping and conforming elements, and the field variables are approximated by finite element shape functions. The meshfree zones are discretized into sets of particles, and the field variables are approximated by meshfree approximations constructed based on the framework of the reproducing kernel particle method (RKPM). An interface constraint is enforced to obtain conforming solutions across the interfaces between zones.
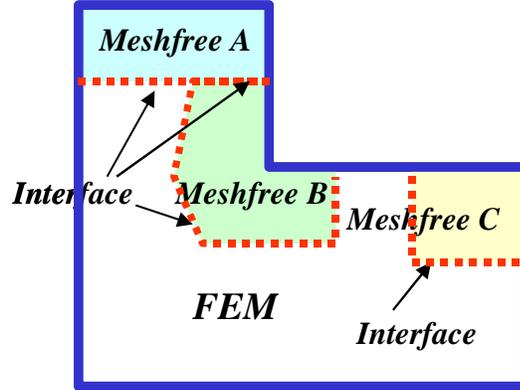
Figure 1 A two-dimensional model of coupled FEM/Mesh-free domain.

The discrete approximation of the field variable $u(x)$ is

$$u^h(x) = \begin{cases} \displaystyle\sum_{\substack{L \\ x_L \in \Omega^i_{FEM}}}^{KP} \Phi_L^{[m]}(x)d_L; \ \forall x \in \Omega^i_{FEM}, \ i=1,...,nf \\[2em] \displaystyle\sum_{\substack{I \\ x_I \in \Omega^j_{meshfree}}}^{IP} \overline{w}_a^{[n]}(x; x - x_I)d_I + \\[2em] \displaystyle\sum_{\substack{L \\ x_L \in \Gamma^{ij}_{Interface}}}^{MP} \Phi_L^{[m]}(x)d_L; \ \forall x \in \Omega^j_{meshfree}, \ j=1,...,nm \end{cases} \qquad (1)$$

In Equation (1), $\Phi_L^{[m]}$ is the standard finite element shape function with interpolation order m and KP is the total number of nodes per element in the finite element zone. Also, $\Gamma^{ij}_{Interface} = \Omega^i_{FEM} \cap \Omega^j_{meshfree}$ for $i=1,...,nf$ and $j=1,...,nm$ is the interface. $\overline{w}_a^{[n]}(x; x - x_I)$ is the reproducing kernel function where n denotes the order of the basis functions and 'a' is the support size of the kernel. $\overline{w}_a^{[n]}$ is defined as

$$\overline{w}_a^{[n]}(x; x - x_I) = H^{[n]^T}(x - x_I)b^{[n]}(x)w_a(x - x_I) \qquad (2)$$

where $H^{[n]}$ is a vector of the nth order monomial basis functions, defined as

$$H^{[n]}(x - x_I) = \left[1, x - x_1, y - y_1, z - z_1, (x - x_2)^2, \cdots, (z - z_2)^n \right]^T \qquad (3)$$

$w_a(x - x_I)$ is a weight/kernel function attached to each particle with its compact support measured by "a". The smoothness of the kernel function defines the smoothness of the reproducing kernel function. A common form of the kernel function utilizes a cubic spline function, which is

$$\phi_a(s) = \frac{1}{6a} \begin{cases} (3s^3 - 6s^2 + 4), & 0 \le s \le 1 \\ -(s-2)^3, & 1 \le s \le 2 \\ 0, & \text{otherwise} \end{cases} \quad ; s = \left|(x - x_I)/a\right| \tag{4}$$

For particle x_I with a support size $\mathbf{a} = [a_1, a_2\, a_3]$, its kernel function is defined as
$\phi_{\mathbf{a}}(\mathbf{x} - \mathbf{x}_I) = \phi_{a_1}((x - x_I)/a_1)\phi_{a_2}((y - y_I)/a_2)\phi_{a_3}((z - z_I)/a_3)$. Various functions can be used to
define the weight/kernel function. LS-DYNA allows users to define the type of spline function
they would like to use and compact support size in the meshfree cards. In Equation (1), *IP* is the
total number of meshfree particles whose kernel supports cover point $\mathbf{x}$, and *MP* is the number
of interface nodes that influence the approximation at point $\mathbf{x}$. In Equation (2), $\mathbf{b}^{[n]}$ is the
coefficient vector, which is so constructed that the *n*th order consistency conditions are satisfied
as:

$$\sum_{\substack{I \\ x_I \in \Omega_{meshfree}}}^{IP} \bar{w}_a^{[n]}(\mathbf{x}; \mathbf{x} - \mathbf{x}_I) x_I^i y_I^j z_J^k$$

$$+ \sum_{\substack{L \\ x_L \in \Gamma_{Interface}}}^{MP} \Phi_L^{[m]}(\mathbf{x}) x_L^i y_L^j z_L^k = x^i y^j z^k, \quad i+j+k=0,\cdots,n \tag{5}$$

Therefore, the coupled approximation of the field variable can be expressed in the following
form

$$\mathbf{u}^h(\mathbf{x}) = \sum_{\substack{I \\ x_I \in \Omega_{Meshfree}}}^{IP} \bar{w}_a^{[n]}(\mathbf{x}; \mathbf{x} - \mathbf{x}_I) d_I$$

$$+ \sum_{\substack{J \\ x_J \in \Gamma_{Interface}}}^{MP} \Phi_J^{[m]}(\mathbf{x}) d_J; \forall\, \mathbf{x} \in \Omega_{Meshfree} \cup \Gamma_{Interface} \tag{6}$$

with *NP* being the total number of mesh-free and interface nodes that influence the solution at
point $\mathbf{x}$ and

$$\bar{w}_a^{[n]}(\mathbf{x}; \mathbf{x} - \mathbf{x}_I) = \Psi_I(\mathbf{x}) -$$

$$\sum_{\substack{J \\ x_J \in \Gamma_{Interface}}}^{MP} \mathbf{H}^{[n]T}(\mathbf{x} - \mathbf{x}_J) \mathbf{M}^{[n]^{-1}}(\mathbf{x}) \mathbf{H}^{[n]}(\mathbf{x} - \mathbf{x}_I) \Phi_J^{[m]}(\mathbf{x}) w_a(\mathbf{x} - \mathbf{x}_I) \tag{7}$$

where $\Psi_I(\mathbf{x})$ is the conventional mesh-free shape function. The moment matrix $\mathbf{M}^{[n]}(\mathbf{x})$ is
defined as

$$M^{[n]}(x) = \sum_{I=1}^{NP} \phi_a(x - x_I) H^{[n]}(x - x_I) H^{[n]^T}(x - x_I) \tag{8}$$

When the finite element interpolation order *m* is equal to the reproducing order *n*, we have

$$\bar{\Psi}_I(x) = 0 \text{ for all nodes } \{I : supp(\Psi_I) \cap \Gamma_{interface} \neq 0\} \text{ and } x \in \Gamma_{interface}. \tag{9}$$

We call Eq. (9) the interface constraint. Now the reproducing kernel function becomes zero for all internal nodes evaluated at interface. If the interface constraint is satisfied, the shape functions on the interface are reduced to the standard finite element shape functions and possess the Kronecker delta property. For the interface between meshfree and meshfree zones, finite element approximation is assumed along the interface. Its interpolation order is chosen to be equal to the reproducing order in two meshfree zones. With the imposition of interface constraints, there are no conforming problems for the shape functions across the interface.

Now consider problems governed by the equations of motion $\rho \ddot{u} = \nabla \cdot \sigma - f_b$ in

$$\Omega = \sum_{i=1}^{nf} \Omega_{FEM}^i \cup \sum_{i=1}^{nm} \Omega_{meshfree}^i \text{ with given boundary and initial conditions. The Galerkin method is}$$

used to convert this set of equations into its corresponding weak form. The coupled meshfree/FE approximation expressed in Equation (1) is introduced to the field variables. The discrete system of equations can then be obtained and solved. For convenience, the domain integration in meshfree computation is performed on the background finite element meshes. Detailed techniques and formulations can be found in LS-DYNA theory manual 2005. Some of its applications in manufacturing process modeling and crashworthiness simulation are reported in [10-13]. The LS-DYNA keywords added for this coupled solver are explained in LS-DYNA Keyword user's Manual.

Numerical Examples

Two crash & safety example problems are employed in the following study. Results from the coupled analyses are compared to ones from the conventional FE analyses.

A European Side Impact Dummy Component Test Simulation

A European side impact dummy component test is simulated. As shown in Figure 2, the dummy is impacted from the left by the door panel. The simulations are performed in IBM workstation p655, AIX 5.1, with four CPUs being used. The original finite element model of the problem is shown in Figure 2(a). The FE analysis fails right after t=23ms due to numerical instability caused by negative element volume of a brick element in upper dummy rib, see Figure 2(b). Using this test, we would like to see the capability of the meshfree formulation in handling large deformation. In the coupled meshfree/FE model, all three ribs are modeled by the meshfree solid formulation defined by *SECTION_SOLID_EFG with element formulation being 41 and dilation parameters being 1.01. The coupled meshfree/FE analysis with this modification failed again due to the element distortion in the dummy jacket. Further on, the dummy jacket is modeled by the meshfree shell formulation defined by *SECTION_SHELL_EFG with element

formulation being 41 and dilation parameters being 1.01. That is, 15966 out of 84,583 nodes are modeled by the meshfree formulations in total. The coupled meshfree/FE analysis is successfully completed. Figure 3(a) shows the coupled meshfree/FE model and Figure 3(b) shows its final deformation.

(a) The FE Model   (b) The deformation at t=20ms
Figure 2 The Finite Element Dummy Side Impact Model

(a)Coupled EFG/FE Model   (b)Deformation at t=60ms
Figure 3 The Coupled meshfree/FE Side Impact Dummy Model
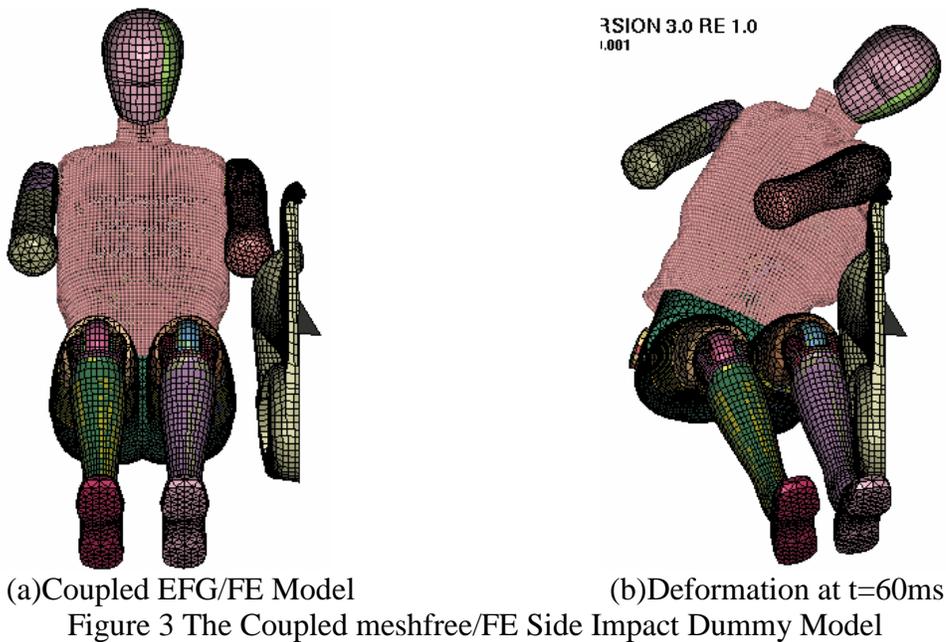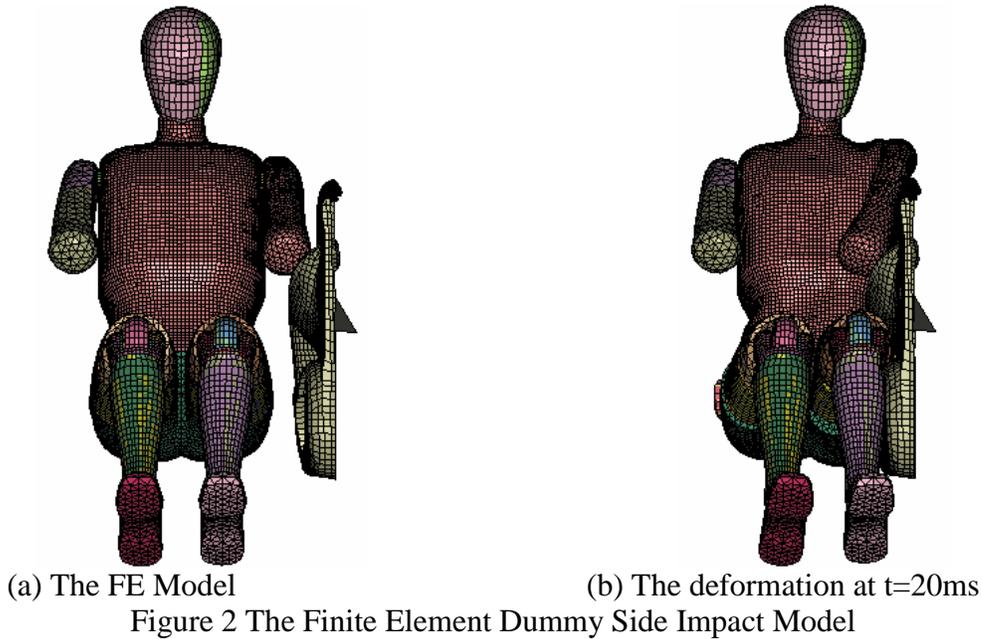
Figure 4 gives the comparison of the response force history. The force curve from the FE analysis shows a sudden raise at the time when the dummy starts to experience excessive deformation, which often contributes to the numerical instabilities. In the FE analysis, negative element volume occurs after this peak and the analysis stops due to numerical instability. In the coupled analysis, no element distortion occurs and the analysis is completed. The response

curves from both analyses agree with each other very well before the distortion occurs. The elapsed CPU time consumed by the FE analysis up to t=23ms is 9083 seconds. For the coupled analysis, the simulation runs up to t=60ms, and 50194 seconds is consumed. The normalized CPU ratio between the FE analysis and the coupled analysis is about 1:2.1 in this testing with 19% nodes modeled by the meshfree formulation.
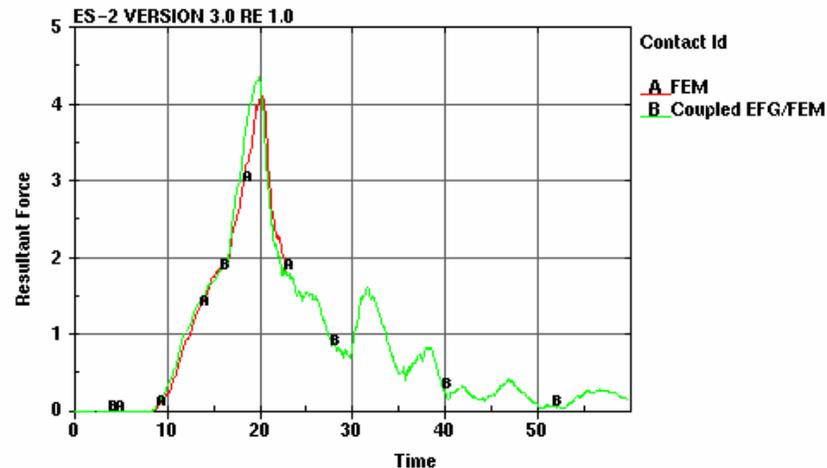
Figure 4 The Response Curve Comparison In The Dummy Component Test

An Engine Cradle Drop Tower Test

An engine cradle drop tower test is to study the cradle response when a cylinder is suddenly dropped onto the cradle. This test is modeled here to investigate the sensitivity of the meshfree solution with respect to different element connectivity since in meshfree computation the element connectivity is still needed to serve as geometry information for domain integration and contact interaction. Two FE models are created: One with the cradle meshed by hexahedral elements as shown in Figure 5(a), and the other is converted from the hexahedral model by splitting each hexahedral element into six tetrahedral elements as shown in Figure 5(b). The cylinder is meshed by hexahedral elements in both models. In the coupled meshfree/FE model, the cradle is modeled by meshfree particles converted from nodes in the FE cradle model, as shown in Figure 5(c), and the element connectivity in the original FE cradle model is used for domain integration and contact interaction. Five simulations were run. They are

   o The finite element analysis of the cradle drop tower test with the cradle meshed by hexahedra with element formulation being 1 in LS-DYNA. That is hexahedral element with one point integration.
   o The finite element analysis of the cradle drop tower test with the cradle meshed by hexahedra with element formulation being 2 in LS-DYNA, the fully integrated S/R solid.
   o The finite element analysis of the cradle drop tower test with the cradle meshed by tetrahedra with element formulation being 10 in LS-DYNA. That is the tetrahedron with one point integration.
   o The coupled meshfree/FE analysis of the cradle drop tower test with the cradle meshed by hexahedral background meshes with element formulation being 41 in LS-DYNA, the meshfree solid.
   o The coupled meshfree/FE analysis of the cradle drop tower test with the cradle meshed by tetrahedral background meshes with element formulation being 41 in LS-DYNA, the meshfree solid.
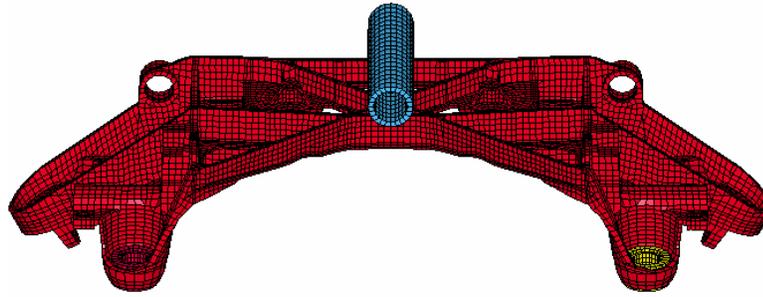
Figure 5(a) The Cradle Model With Hexahedral Mesh
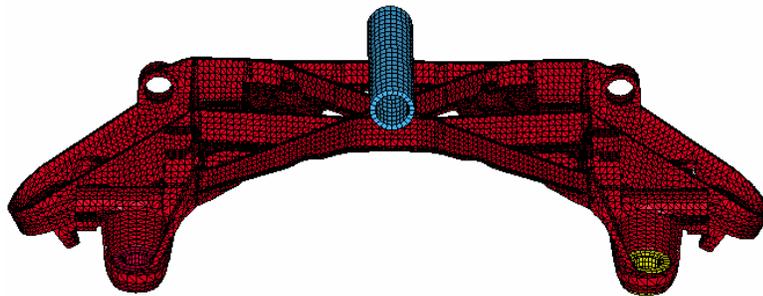
Figure 5(b) The Cradle Model With Tetrahedral Mesh
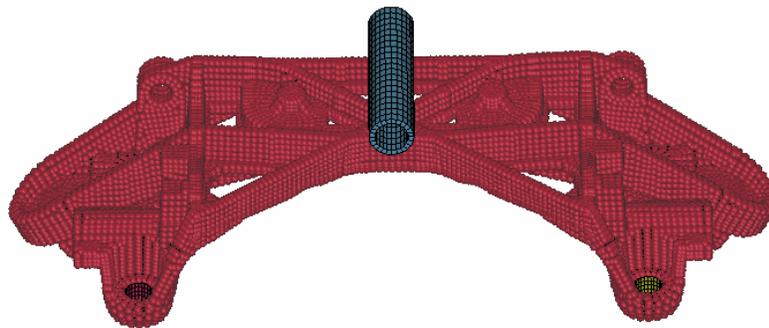
Figure 5(c) The Cradle Modeled By Meshfree Particles

The deformed shape of the cradle modeled by meshfree particles with hexahedral background mesh is shown in Figure 6. The response curves from the five simulations are plotted in Figure 7. The response curves show that the FE analysis with tetrahedral mesh yields very stiff result. The FE analysis with hexahedral mesh and one point integration yields very soft result. The FE analysis with hexahedral mesh and full integration leads to a result in between. In theory, this result should be more accurate than the results from one point domain integration since fully integrated element formulation performs well for this type of small deformation problem. The meshfree analysis with tetrahedral background mesh and the meshfree analysis with hexahedral background mesh lead to very similar results. The result from tetrahedral background mesh seems a little bit stiffer than the one from hexahedral background mesh. Both results are close to

the one from the fully integrated hexahedral FE model. The difference in the results of two meshfree analyses is because current meshfree formulation relies on background meshes to do domain integration and contact detection. Table 1 gives the normalized CPU consumption of the five tests. Since a majority of the model is modeled by the meshfree formulation, the two coupled meshfree/FE analyses consume significantly higher CPU than the FE analyses.
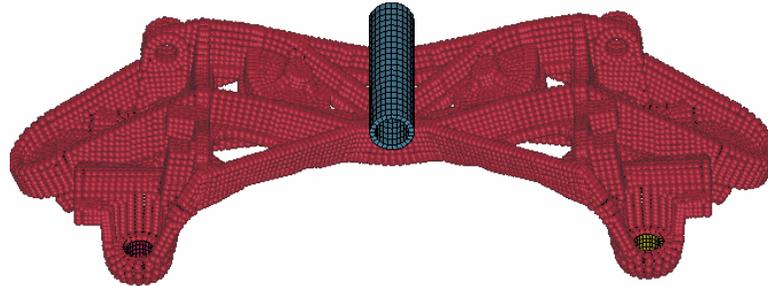
Figure 6 The Deformed Shape Of Cradle From The Coupled Analysis
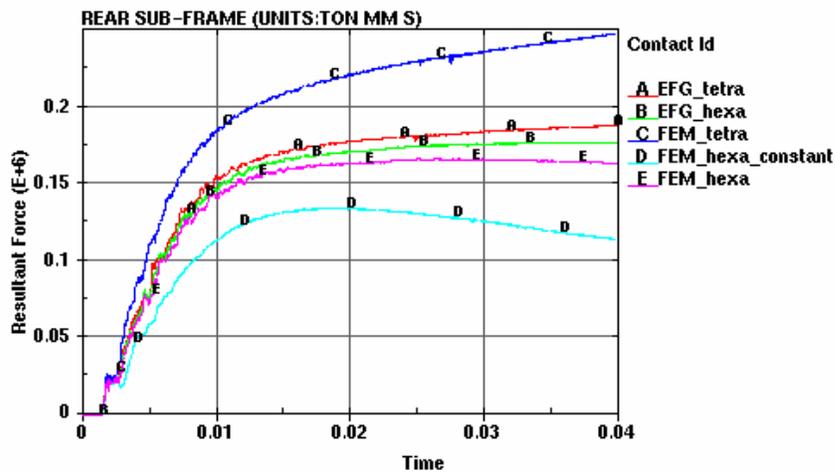
Figure 7 The Response Curve Comparison Of The Cradle Drop Tower Problem

Table 1 The Normalized CPU Consumption Of The Five Simulations Of Cradle Drop Tower Test

	FEM with Hexa 1	FEM with Hexa 2	FEM with Tetra 10	Meshfree with hexa	Meshfree with tetra
Normalized CPU	1	2.5	3.0	12	21.0

Summary

This paper applies a newly developed coupled meshfree/finite element analysis tool in LS-DYNA for the analysis of crash & safety problems. Two problems are employed. They are a European side impact dummy component test and an engine cradle drop tower test.

In the first problem, the dummy is impacted from the left side by a door panel. The mesh-based model analysis shows excessive element deformation in the upper rib foam of the dummy when the door panel pushes onto the dummy. Negative element volume occurs, leads to numerical instabilities and hence fails analyses. Then, by modeling the rib foams and dummy jacket with the meshfree particles, the analysis is successfully completed. The coupled analysis consumes about twice of CPU time as what the finite element analysis does. The second problem is an engine cradle drop tower test used to test the sensitivity of the meshfree solution with respect to the different background meshes. For the same spatial domain discretization, the finite element analysis gives very different solutions for different element connectivity. The hexahedral mesh with one point integration gives an unrealistic soft response. The tetrahedral mesh results in a very stiff solution. Instead, the meshfree analysis with the hexahedral background mesh and the meshfree analysis with the tetrahedral background mesh yield very similar results, which agree well with the result from the FE analysis of the hexahedron model with full integration.

The above two testing problems show that the coupled meshfree/finite element models are numerically more stable in dealing with large deformation than the finite element models. Also, they are less sensitive to the change in element connectivity. The increase in required computer resource is limited when only the problematic area is switched to meshfree particles. It is also worthwhile to spend this extra time to gain the big savings in running multiple analyses in a trial-and-error fashion to find a numerically stable solution. Based on this study, the coupled meshfree/FE method provides a robust tool for simulating analyses involving excessive distortion of solid elements.

Acknowledgments

References

1. Randles, P. W., and Libersky, L. D., "Smoothed particle hydrodynamics: some recent improvements and applications," Comput. Methods in Applied Mechanical Engineering, 139, 375–408, 1996.
2. Belytschko, T., Lu, Y. Y., and Gu, L., "Element free Galerkin method," Int. J. Num. Methods Eng., 37, 229–256, 1994.
3. Liu, W. K., Jun, S., and Zhang, Y. F., "Reproducing kernel particle methods," Int. J. Num. Methods in Fluids, 20, 1081–1106, 1995.
4. Chen, J. S., Pan, C., Wu, C. T., and Liu, W. K., "Reproducing kernel particle methods for large deformation analysis of nonlinear structures," Comput. Methods Appl. Mech. Eng., 139, 195–227, 1996.
5. Melenk, J. M., and Babuska, I., "The partition of unity finite element method: basic theory and applications," Computational Methods in Applied Mechanical Engineering, 139, 289–314, 1996.
6. Duarte, C. A. M., and Oden, J. T., "A H–P adaptive method using clouds," Comput. Methods Appl. Mech. Eng., 139, 237–262, 1996.

7. Krongauz Y, Belytschko T., "EFG Approximation With Discontinuous Derivatives," International Journal For Numerical Methods In Engineering 41 (7): 1215-1233, April 1998.

8. Fleming M, Chu YA, Moran B, Belytschko T., "Enriched Element-Free Galerkin Methods For Crack Tip Fields," International Journal For Numerical Methods In Engineering 40 (8): 1483-1504, April 1997.

9. Huerta, A. and Fernandez-Mendez S., "Enrichment and Coupling of the Finite Element and Meshless Methods," International Journal For Numerical Methods In Engineering, Vol. 48, pp 1615-1636, 2000.

10. Wang, H. P., Zhao, Kunmin, Wu, Cheng-Tang and Botkin, M. E., "Mesh-Free Simulation Of Automotive Decklid Inner Panel," Proceedings of Numisheet2005: 6th International Conference and Workshop on Numerical Simulation of 3D Sheet Metal Forming Processes, August 15 – 19, 2005, Detroit, Michigan, USA.

11. Wang, H. P. and Cheng, Y. P., "Modeling Sid-Iis Dummy Shoulder Using A Coupled Meshfree/Finite Element Tool," Proceedings of McMat2005: 2005 Joint ASME/ASCE/SES Conference on Mechanics and Materials, June 1 – 3, 2005, Baton Rouge, Louisiana, USA.

12. Wu, C. T., Guo, Y., Wang, H. P. and Botkin, M. E., "A Meshfree Analysis of Shell Structures," Proceedings of 8th LS-DYNA user conference, Detroit 2004.

13. Guo, Y., Wu, C. T., Botkin, M. E. and Wang, H. P., "Coupled FEM/Mesh-Free Shear-Deformable Shells for Nonlinear Analysis of Shell Structures," Proceedings of WCCM VI in conjunction with APCOM'04, Sept. 5-10, 2004, Beijing, China.